Origin, Metamorphic History, and Tectonic Setting of Archean Rocks from the Spuhler Peak Assemblage, Tobacco Root Mountains, MT

Chris Poulsen
Carleton College
Northfield, MN 55057

Introduction

The Spuhler Peak Assemblage's distinct lithologies stand out among the other lithological units of the Tobacco Root Mountains, located structurally above and below the Spuhler Peak Assemblage. Unlike the Indian Creek Metamorphic Suite (ICMS) and the Pony-Middle Mountain Metamorphic Suite (PMMMS) which are dominated by meta-sedimentary and meta-plutonic rocks, the Spuhler Peak Assemblage contains large quantities of amphibolite with smaller amounts of meta-sedimentary, meta-ultramafic, and other amphibole-rich rocks. These lithological differences between units of the Tobacco Root Mountains raise some interesting questions about the relationships between units. The goal of this project is to shed some light on the relationship between the Spuhler Peak Assemblage and the ICMS and PMMMS.

In this study, I examine the field relationships, petrology, and geochemistry of a suite of rocks exposed along Branham and Leggat Ridge, situated at the southeastern most portion of the Spuhler Peak Assemblage. My goal is to characterize the rocks in this suite, revealing their parent rocks, metamorphic history, and Archean tectonic setting. Additionally, I focus on the ultramafic rocks found throughout the Spuhler Peak Formation. These rocks have received little attention, but are potentially very important for understanding the tectonics of the region.

Field Relationships

Both Branham Ridge and Leggat Ridge contain good exposures of Spuhler Peak lithologies. They trend northeast-southwest, though a small portion of Leggat Ridge trends nearly east-west. Foliations along the ridges are fairly constant, striking to the northwest and dipping moderately to steeply (45-85°) to the northeast. The only significant deviation is caused by an isoclinal fold on Leggat Ridge.

The Spuhler Peak Assemblage, as exposed on Leggat and Branham ridges, includes interlayered amphibolite, hornblende-plagioclase-quartz gneiss, other amphibole-rich rocks, quartzite, sillimanite-bearing quartz-plagioclase-garnet-biotite schist. Lithologies vary greatly in thickness (<1m to more than 300m) and are commonly discontinuous or covered by talus, making mapping of individual lithologies nearly impossible. In order to determine relationships between the lithologies, I measured their thicknesses perpendicular to the foliation along the Spuhler Peak and Branham ridges. (See figures 1 and 2.)

In contrast to the interlayered lithologies, the meta-ultramafic rocks occur as layers and pods with thicknesses from 10 to 20 meters and lengths from 10 to a few hundred meters. The longer meta-ultramafic bodies are conformable to compositional layering in the amphibolite (Cummings and McCulloch, 1989). The meta-ultramafics are separated from adjacent amphibolite by a reaction rim of black hornblende gneiss. However, at two exposures (one within my field area and one on Spuhler Peak Ridge) the contact is zoned and includes hornblende, actinolite, biotite, and chlorite-rich layers.

The other amphibole-rich rocks are found in a variety of relationships. On Branham Ridge, they occur as a massive, discontinuous unit. They are also found adjacent to amphibolite and pelitic rocks on Leggat Ridge and in the valley separating Leggat Ridge from Branham Ridge. In these occurrences, there is no sharp contact between lithologies. The amphibolite and pelitic rocks grade into the other amphibole-rich lithologies which are less than a meter thick.

Petrography

Amphibolites. Amphibolite may be a misnomer, since the rocks in this category are not always dominated by hornblende and plagioclase. These rocks are dark colored and show either a salt and pepper texture or leucocratic stringers of quartz and plagioclase, in which case they are probably better referred to as hornblende-plagioclase-quartz gneiss. Hornblende is the main component of these rocks, varying in concentration from 30 to 70%, and plagioclase is an important component, making up 5-40% of the bulk composition. Quartz and garnet are abundant in the hornblende-plagioclase-quartz gneiss, varying between 5 to 40% and 0 to 24%, respectively. Minor minerals include opaques, epidote, chlorite, talc, actinolite, apatite, zircon, biotite, and spinel. Some of these rocks have a weak foliation with garnets commonly exhibiting fractures perpendicular to foliation.

Quartzites and Quartzofeldspathic schist . Siliclastic metamorphic rocks range in composition from a nearly pure quartzite (93% quartz) to a sillimanite-bearing, plagioclase-quartz-garnet-biotite gneiss. These rocks are dominated by quartz (30-93%), plagioclase (0-40%), biotite (1-50%), and garnet (0-40%). Minor components include sillimanite (1-10%), chlorite (<1%), muscovite (<1-3%), opaques (<1%), phlogopite (1%), and zircon (<1%). Two forms of sillimanite are present, a slender prismatic form and a fibrolitic form. The slender prismatic form of sillimanite is uncommon and probably originated at higher pressures and temperatures than the fibrolite form (Yardley, 1989). Pelites exhibit a strong foliation and are compositionally banded into quartzofeldspathic layers and biotite-garnet-sillimanite layers with smaller amounts of quartz and plagioclase.

Meta-ultramafics. The meta-ultramafic rocks are dark green and gray rocks, and vary from fine-grained to very coarse-grained. The meta-ultramafics differ considerably in the amount of metamorphic alteration they have undergone, with one sample composed of 70% talc and other samples devoid of talc. Relict olivine and relict orthopyroxene (up to 1 cm) are present in all of the samples, though usually not together in the same sample. Tremolite-actinolite replaces the olivine and orthopyroxene. Other minerals common in the meta-ultramafics are chlorite, opaques, and rutile. Foliation is poorly developed, although chlorite usually shows a preferred orientation.

Hornblende gneiss. As mentioned above, these rocks surround the meta-ultramafics at their contact with the amphibolites. They are easily recognizable by their black color and coarse grain size (up to 8-9 cm). Hornblende (97-98%) is the principal mineral, but minor amounts of plagioclase, quartz, chlorite, opaques, epidote, garnet, and apatite are present.

TABLE 1. Major elements (in oxide weight percents) and trace elements (in ppm). Locations are Spuhler Peak area (SP), Indian Ridge (IR), Mustard Pass area (MP), Gneiss Lake Area (GL), and Branham Lakes area (BL). * all iron as FeO.

Sample	1	2	3a	4	5	6b	7	11	12	13	14	15
SiO2	56.68	47.83	51.65	47.67	53.64	45.99	44.83	59.15	55.89	50.79	47.25	52.7
Al2O3	15.45	14.79	14.34	13.52	7.421	15.39	14.25	18.25	14.79	13.55	13.25	14.32
FeO*	8.72	12.84	14.68	15.96	12.38	17.15	17.71	9.205	10.75	16.17	12.93	14.92
MgO	5.258	9.597	8.5	12.77	17.41	11.18	12.85	5.86	5.884	6.187	18.72	8.673
CaO	3.258	1.708	2.235	1.886	1.883	1.519	1.698	.3458	4.095	6.739	1.149	2.622
Na2O	6.844	4.013	2.521	2.938	1.322	1.971	1.361	.4352	3.614	.8216	1.443	1.904
K2O	.4727	2.576	.476	.6653	.9902	1.395	.1364	2.894	.5242	.5611	.622	2.256
MnO	.1557	.1971	.3366	.0981	.1362	.1373	.2181	.2128	.2057	.2427	.1351	.1937
P2O5	.1173	.1402	.2884	.2729	.1252	.2352	.3787	.0649	.1981	.231	.124	.0934
TiO2	.9798	1.255	1.323	1.33	.8389	1.884	2.014	.725	.8254	2.035	.6964	.3847
Ba	74.07	493.4	32.54	121.4	85.81	229.6	33.94	463.4	155.4	146.5	23.05	252.6
Cr	106.1	139.2	94.01	21.01	705.3	83.4	47.39	368.4	115.5	189.2	611.7	2543
Be	1.041	1.061	1.309	1.742	.9689	.6042	.7367	.7099	2.398	1.874	1.429	1.026
Ce	27.6	30.73	57.23	74.3	39.44	37.47	95.32	33	44.49	33.09	37.11	17.89
Co	32.12	64.48	38.46	55.02	67.77	55.74	46.12	34.85	39.56	48.62	65.24	99.85
La	7.617	5.198	24.64	33.49	16.44	11.19	72.91	10.57	21.84	.3613	16.14	6.214
Ni	73.4	147.2	21.51	20.86	724.7	101.3	25.41	155.7	61.59	90.88	167.8	775.9
Sc	29.94	33.19	43.33	32.83	19.24	33.99	69.3	20.17	34.73	41.87	37.27	39.42
Sr	74	49.81	33.42	47.39	33.89	36.55	17.58	12.17	117	41.04	8.776	76.58
V	202.6	294	279.6	337.1	131.4	269.4	293.2	149.9	209.9	394.1	208.8	182.2
Y	17.93	21.49	52.87	30.71	20.1	37.9	75.66	13.91	30	36.26	20.38	19.29
Yb	1.813	1.762	5.527	2.892	2.182	3.739	10.39	1.378	3.197	2.419	2.32	2.359
Zr	101	110.1	136.6	283	153.5	173.5	153.7	154.8	147.8	137.2	123	68.43
Area	IR	IR	IR	SP	SP	SP	SP	IR	IR	IR	IR	MP

Sample	16	17	18	20	21	26	27	29a	29b	29c	30
SiO2	48.93	63.1	54.73	55.82	51.07	50.19	49.06	48.87	53.23	54.93	50.4
Al2O3	13.64	10.16	15.14	12.5	13.97	13.78	13.7	14.08	15.12	14.83	13.32
FeO*	11.8	7.603	13.24	9.442	11.45	18.12	12.64	13.77	13.19	11.49	13.4
MgO	11.79	11.01	6.048	10.14	5.854	7.476	12.04	6.841	6.343	5.891	12.83
CaO	7.97	.6718	3.266	6.544	7.769	2.952	4.672	8.293	4.684	4.97	1.322
Na2O	1.701	1.194	3.081	2.377	3.549	2.185	2.866	2.641	4.493	3.769	2.155
K2O	1.35	.8442	.4488	.5264	.6762	.4791	1.035	.834	.4931	.6876	.5643
MnO	.262	.0376	.2357	.01334	.1955	.3951	.2516	.228	.1797	.1756	.1071
P2O5	.0732	.2395	.3665	.123	.3777	.1919	.0914	.1546	.1571	.4123	.3142
TiO2	.3289	.9145	1.557	.6108	1.46	1.113	.6856	1.073	1.215	1.467	1.376
Ba	115.5	21.01	49.82	39.12	287.7	54.96	62.96	124.7	81.88	125.1	25.46
Cr	1247	30.35	48.9	605.4	59.8	73.6	49.81	113.5	104.7	55.23	96.65
Be	1.159	1.213	2.209	1.246	2.463	1.021	1.238	2.195	1.506	2.668	2.233
Ce	29.73	36.96	72.59	25.41	76.73	36.48	10.75	23.32	27.5	50.83	40.31
Co	59.57	26.23	41.57	48.21	43.61	54.5	45.81	54.59	56.04	37.66	48.11
La	16.15	19.44	42.74	17.28	50.62	22.95	1.541	14.87	10.33	30.41	19.3
Ni	349.3	22.65	25.43	141.2	61.87	72.84	40.13	79.58	103.3	27.73	33.56
Sc	39.92	24.85	44.08	32.5	35.93	36.01	36.65	45.12	36.97	38.39	38.13
Sr	39.04	10.78	90.45	41.66	113.7	29.99	50.88	93.03	113	118.6	27.92
V	178.6	190.2	313	183.6	263.2	211.8	225.7	295.4	282.2	290.3	307.4
Y	19.54	34.17	50.66	20.09	50.25	35.04	18.26	30.47	27.44	43.55	30.56
Yb	2.42	3.873	5.543	2.48	5.485	3.727	1.827	3.142	2.482	4.328	3.004
Zr	45.31	206.4	289.2	109.6	344.4	244.3	93.38	177.4	208	425.5	415.6
Area	MP	MP	MP	IR	IR	SP	GL	BL	BL	BL	RL

REFERENCES CITED

Burger, H. R., 1966, Structure, petrology, and ecconomic geology of the Sheridan district, Madison County, Montana [Ph.D. thesis], Bloomington, Indiana, Indiana University, 156 p.

Cattell, A. C., and Taylor, R. N., 1992, Archaean basic magmas, *in* Hall, R. P. and Hughes, D. L., eds., Early Precambrian basic magmatism: Glasgow, Great Britain, Blackie, p. 12-39.

Cummings, M. L., and McCulloch, W. R., 1992, Geochemistry and origin of amphibolite and ultramafic rocks, Branham Lakes area, Tobacco Root Mountains, southwestern Montana, *in* Bartholomew, M. J., Hyndman, D. W., Mogk, D. W., and Mason, R. eds., Basment Tectonics 8: Characterization and comparison of ancient and Mesozoic continental margins - Proceedings of the 8th International Conference on Basement Tectonics (Butte, Montana, 1988): Dordrecht, The Netherlands, Kluwser Academic Publishers, p. 323-340.

Gillmeister, N. M., 1971, Petrology of Precambrian rocks in the central Tobacco Root Mountains, Madison County, Montana [Ph.D. thesis]: Cambridge, Massachusetts, Harvard University, 210 p.

Humphris, S. E., and Thompson, G., 1978a, Hydrothermal alteration of basalts by seawater: Geochimica et Cosmochimica Acta, v. 42, p. 107-125.

Humphris, S. E., and Thompson, G., 1978b, Trace element mobility during hydrothermal alteration of oceanic basalts: Geochimica et Cosmochimica Acta, v. 42, p. 127-136.

Irvine, T. N., and Baragar, W. R. A., 1971, A guide to the chemical classification of the common volcanic rocks: Canadian J. of Earth Sci., v. 8, p. 523-548.

Jensen, L. S., 1976, A new cation plot for classifying subalkalic volcanic rocks: Ontario Div. Mines, MP 66, 22p.

MacGeehan, P. J., and MacLean, 1980, An Archean sub-seafloor geothermal system, 'calc-alkali' trends, and massive sulfide genesis: Nature, v. 286, p. 767-771.

O'Neill, J. M., 1983, Geologic map of the Middle Mountain - Tobacco Root roadless area, Madison County, Montana: US Geological Survey Miscellaneous Field Studies Map MF-1590A.

Pearce, J. A., and Cann, J. R., 1973, Tectonic setting of basic volcanic rocks determined using trace element analyses: Earth Planet. Sci. Letters, v. 19, p. 290-300.

Reinhardt, J., 1987, Cordierite-anthophyllite rocks from north-west Queensland, Australia: metamorphosed magnesian pelites: Journal of Metamorphic Geology, v. 5, p. 451-472.

Robinson, P, Spear, F. S., Schumaker, J. C., Laird, J., Klein, C., Evans, B. W., and Doolan, B. L., 1982, Phase realtions in metamorphic amphiboles: natural occurence and theory, *in* Veblen, D. R., and Ribbe, P. H., eds., Amphiboles, minerology and experimental phase relations: Mineralogical Society of America, v. 9B, p. 1-211.

Sun, S. S., 1984, Geochemical Characteristics of Archaean Ultramific and Mafic Volcanic Rocks: Implications for mantle composition and evolution, *in* Kroner, A., Hanson, G. N., and Goodwin, A. M., eds., Archaean Geochemistry: Berlin, Germany, Springer-Verlag, p. 25-46.

Vitaliano, C. J., and Cordua, W. S., Comp., 1979, Geologic Map of the Southern Tobacco Root Mountains, Madison County, Montana: Geological Society of America Map and Chart Series MC-31, scale 1:62,500.

Other amphibole -rich rocks. The outstanding feature that holds this category together is the presence of dark, elongated amphiboles that range in size from less than one centimeter to several centimeters. Though normally brown, one rock included in this group contains a green, radiating amphibole. Mineralogically, geochemically, and geographically these rocks vary considerably. Several samples are composed almost exclusively of amphiboles, whereas other samples contain large amounts of quartz, plagioclase, and garnet. The dominant amphibole is tremolite, but a second amphibole, such as actinolite, hornblende, anthophyllite, or gedrite, is normally present in smaller quantities. In some places, tremolite appears to be pseudomorphed by a colored, pleochroic amphibole, either hornblende or actinolite. Minor minerals include opaques, zircon, biotite, chlorite, apatite, talc, and spinel.

Geochemistry

I employed Carleton's Philips 1404 X-ray Fluorescence Spectrometer (XRF) to calculate the major element chemistry of the meta-ultramafic, amphibolite, hornblende-plagioclase gneiss, hornblende gneiss, and other amphibole-rich lithologies. Additionally, I sent ten samples to XRAL Laboratories to obtain trace element and rare earth element chemistry. An X-Ray Fluorescence Spectrometer (XRF) derived trace element concentrations, an Induced Coupled Plasma Mass Spectrometer (ICPMS) calculated rare earth element concentrations. On the basis of weight % of MgO , these rocks break into two distinct clusters. The meta-ultramafic lithologies are clearly enriched in MgO. The amphibolites, hornblende-plagioclase gneiss, and hornblende gneiss have intermediate MgO concentration.

With weight % of MgO averaging 27.2, the meta-ultramafic rocks are clearly candidates for characterization as komatiites. Additionally, these rocks have relatively high CaO:Al_2O_3 (.72-1.54 wt.%) ratios, low SiO_2 concentrations (<50 wt.%), and low TiO_2 concentrations (<.31 wt.%). There is some debate as to how high komatiitic CaO:Al_2O_3 ratios should be, Arndt and Nisbet (1982) suggest that the ratio be roughly equal to or greater than one. The meta-ultamafic rocks are enriched in nickel (1120-1290 ppm) and chromium (2450-2790 ppm) and depleted in yitrium (2-8 ppm) and zirconium (25-41 ppm).

Amphibolite and hornblende-plagioclase-quartz gneiss are characterized by the following average major element concentrations: MgO (5.52-9.96 wt.%), Al_2O_3 (12.3-15.46 wt.%), Na_20 (.78-2.46 wt.%), CaO (5.4-12.93 wt.%), and Fe_2O_3 (8.34-16.9 wt.%). The major element chemistry plots in the tholeiitic basalt field on discrimination diagrams. (See figures 3 and 4.) The amphibolite and hornblende-plagioclase-quartz gneiss are depleted in chromium (8-109 ppm) and nickel (45-99 ppm) and slightly enriched in yitrium (10-26 ppm) and zirconium (34-85 ppm).

The major element chemistry of the other amphibole-rich rocks varies dramatically from sample to sample. For example, SiO_2 ranges from 41.9 to 55.86 wt.%, MgO varies from 9.25 to 25.04 wt.%, and CaO spreads from 2.26 to 10.4 wt.%.

Discussion

Geochemical and petrological data suggest that the meta-ultramafic rocks are derived from a komatiitic suite. Earlier workers interpreted the ultramafic pods in the Tobacco Root and Ruby Mountain Ranges as diapiric serpentinites derived from the alteration of peridotites (Mogk et al., 1989, Desmarais, 1980). A comparison of the major element chemistry of the meta-ultramafic rocks and known peridotites, however, does not support this interpretation for the meta-ultramafics in the Tobacco Root Mountains. (See figure 5, 6, 7, 8.) Cummings and McCullough (1989) argue that the megacrysts of olivine and pyroxene and lack of relic spinifex are not consistent with a komatiitic parentage. However, there is some question as to whether a spinifex texture could be preserved after exposure to upper amphibolite facies metamorphism. Though the meta-ultramafics may not be strictly defined komatiites due to the absence of extrusive features, evidence suggests that they were part of a komatiitic flow, perhaps as cumulates at the base of a flow or feeder dikes for overlying flows.

The protolith of the amphibolite rocks is most likely a tholeiitic basalt. Both the geochemical and petrographic data indicate such an origin. Discrimination diagrams using Ti- Zr-Y and Ti- Zr-Sr are not conclusive as to the Archean tectonic setting of the amphibolites, offering ocean island basalts, continental basalts, ocean floor basalts, and low-potassium basalts as potential parent rocks. (See figures 9 and 10.) The mineralogy of the amphibolites provides some information about their past metamorphic conditions. One sample contains an assemblage of clinopyroxene, orthopyroxene, hornblende, plagioclase, quartz, and relict garnet. McBirney (1989) indicates this assemblage is indicative of the granulite facies under medium pressure. Exposure of the amphibolites to the greenschist facies is recorded by the varying amounts of actinolite, talc, epidote, chlorite, and garnet present in the rocks. The dominance of minerals associated with the greenschist facies is good evidence that this metamorphic phase was a retrograde event and not a preserved prograde event.

The other amphibole-rich rocks have probably undergone hydrothermal alteration. Their geochemistry varies considerably and does not correspond with any common parent rock type. Consideration of their mineralogy and location suggests that they were initially ultramafics, tholeiitic basalts, or arenaceous sediments before their alteration.

The quartzite and quartzofeldspathic schist were originally sandstones and arenaceous sediments. The presence of two forms of sillimanite in some of these rocks may indicate two phases of metamorphism, one event at upper-amphibolite to granulite facies and a second event at amphibolite facies. The paucity of the prismatic form of sillimanite relative to its fibrous form suggests that the amphibolite facies metamorphism was probably a retrograde event.

The tectonic setting of the Spuhler Peak Assemblage is not easily constrained due partially to the fact that Archean tectonics are not well understood. Although Mogk et al. (1989) interpret the Archean history of southwestern Montana in modern plate tectonic terms, the Spuhler Peak Assemblage might not have a modern day analog. However, using the evidence collected in this paper, I propose a tentative tectonic model for the Spuhler Peak Assemblage. The presence of small quantities of komatiite with tholeiitic basalts, sandstones, and arenaceous sediments suggests that these lithologies might have erupted from or were deposited in a rifting continental basin. The absence of deep sea sediments indicates rifting did not progress far before regional compression began, closing the basin, and eventually thrusting the basinal deposits over the sedimentary rocks of the ICPMS.

Figure 1 and 2. Stratigraphic columns illustrate the lithologies exposed along Leggat Ridge and Branham Ridge from the northeast (bottom) to the southwest (top).

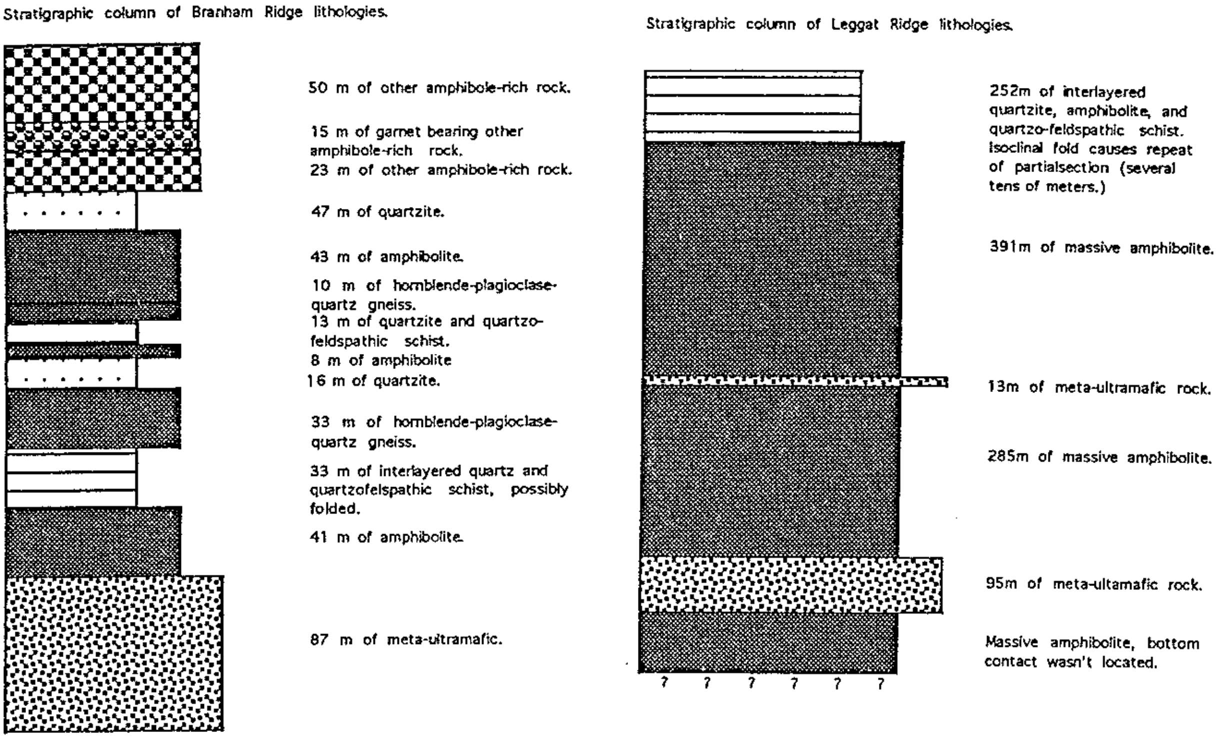

Figures 3 and 4. These differentiation diagrams show that the amphibolites and hornblende-plagioclase-quartz gneisses clearly plot in the tholeiitic basalt field.

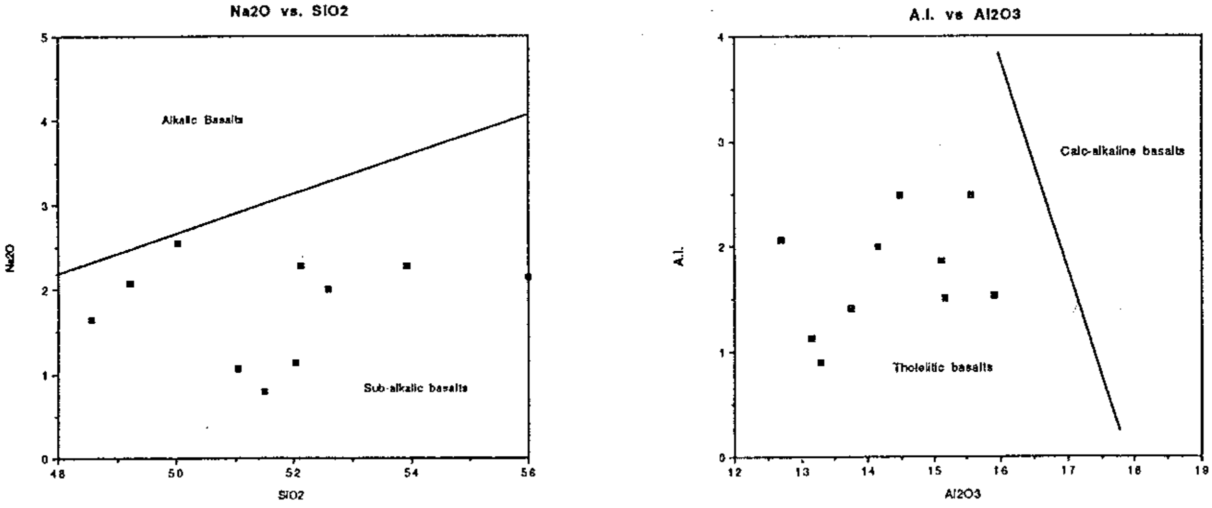

References

Arndt, N.T., and E.G. Nisbet, 1982, What is a komatiite?; pp. 19-27 in N.T. Arndt and E.G. Nisbet (eds.), Komatiites: George Allen & Unwin, London, England, UK, 539 p.

Cummings, M.L. and W.R. McCulloch, 1989, Geochemistry and origin of amphibolite and ultramafic rocks, Branham Lakes area, Tobacco Root Mountains, southwestern Montana: International Basement Tectonics Association No. 8, p. 323-340.

Desmarais, N., 1981, Precambrian metamorphic rocks in the Ruby Range, Montana:Precambrian Research, v. 16, p. 67-101.

Herzberg, C.T., 1993, Lithosphere peridotites of the Kaapvaal Craton: Earth and Planetary Science Letters, 120, p. 13-29.

Mogk, D.W., P.A. Mueller, J.L. Wooden, and D.R. Bowes, 1989, The northern Wyoming Province: Contrasts in Archean crustal evolution, International Basement Tectonics Association No. 8, p. 283-297.

Yardley, B.W.D, 1991, Metamorphic Petrology, Longman Scientific & Technical, New York, New York, 248 p.

Figures 5, 6, 7, and 8. Differentiation diagrams illustrate that the meta-ultramafics consistently fall in the komatiite field and not the peridotite field. Amphibolites are plotted to show distinct chemical differences between meta-ultramafics and amphibolites (Crosses are meta-ultramafics, filled boxes are amphibolites and hornblende-plagioclase-quartz gneisses.)

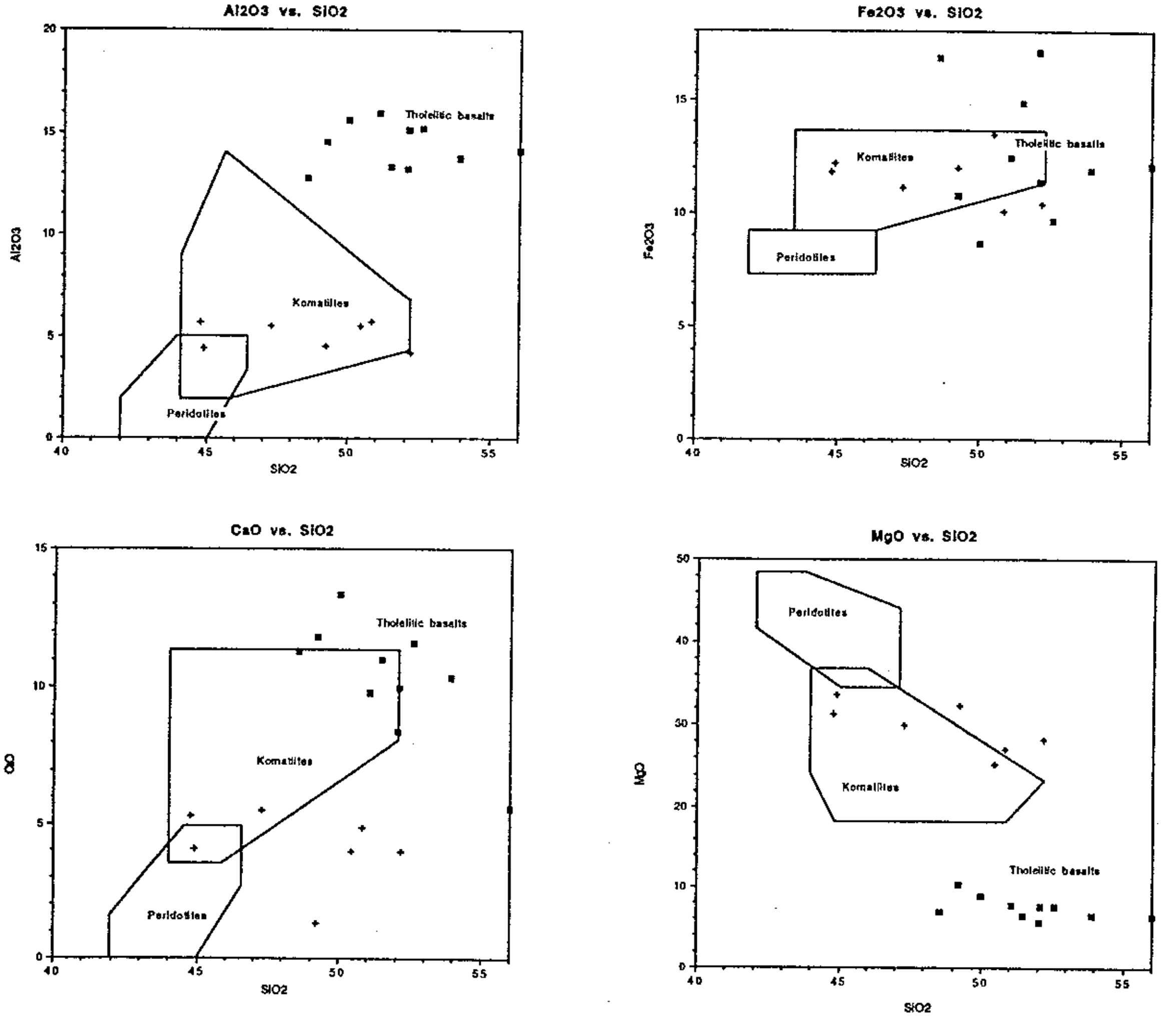

Diagram 9 and 10. Amphibolites plot in three different fields on the Ti-Zr-Y and Ti-Zr-Si ternary diagrams, offering ocean island basalts, continental basalts, ocean floor basalts, and low-potassium basalts as possible parent rock types.

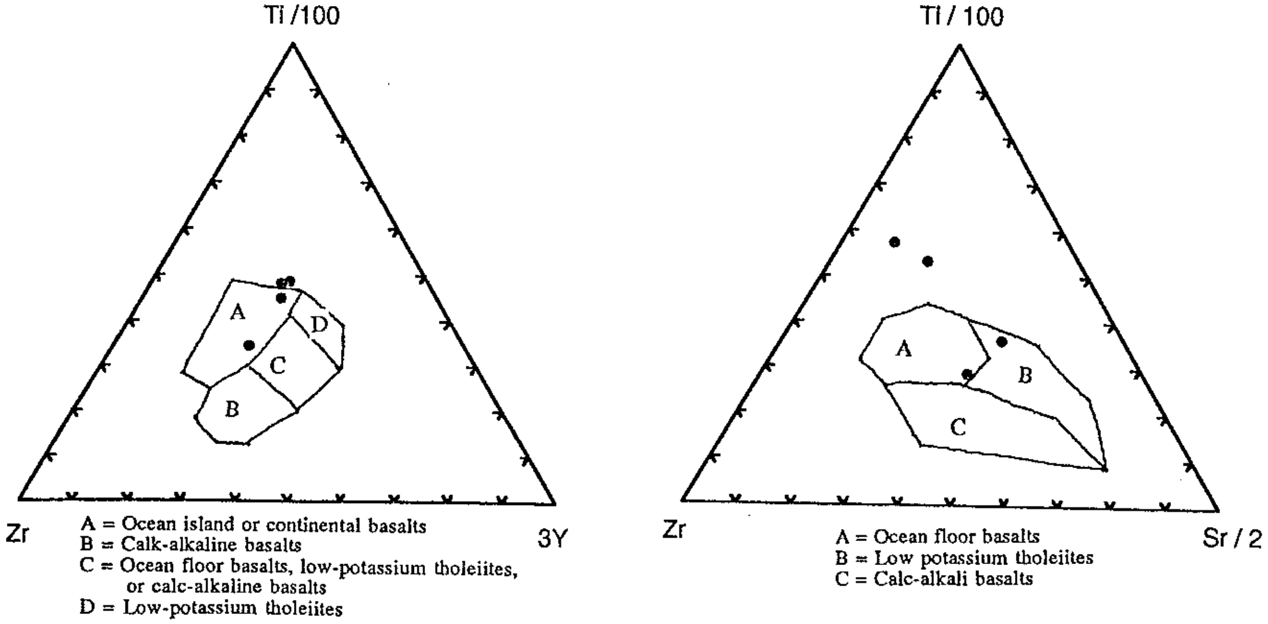

Structural and Metamorphic History of an Intensely Deformed Zone, Lower Branham Lake, Southern Tobacco Root Mountains, Montana

Mary Jennifer Sincock
Department of Geosciences
Franklin and Marshall College
Lancaster, Pennsylvania

Introduction: The purpose of this study was to describe the structural and metamorphic history of an intensely deformed zone within the Spuhler Peak Formation near Lower Branham Lake in the Southern Tobacco Root Mountains, Montana (Figure 1). These Archean rocks have undergone upper amphibolite to granulite prograde metamorphism and a late minor greenschist retrograde metamorphism (Burger, 1967; Wooden and others, 1988).

Field Observations: The area contains an intensely deformed metasedimentary package enveloped by a massive amphibolite package, with metaultramafic pods present throughout. An offshoot granodiorite plug of the Late Cretaceous Tobacco Root Batholith cuts across these rock units (Figure 1). In both metasedimentary and amphibolite packages, foliations are oriented approximately N50°W; 60°NE. Contacts between the packages are parallel to the foliations and are folded in some places. Within the intensely folded metasedimentary package three generations of folds were recognized. The metasedimentary package also includes an intensely recrystallized metamylonite (?) zone.

Analytical Techniques: Sixty-two oriented samples were collected in the field; from these twenty-nine thin sections were cut and analyzed. Sixteen samples were selected for whole rock chemical analysis. X-ray fluorescence, inductively coupled plasma, and loss on ignition techniques were used to determine major and trace element compositions. Whole rock chemical compositions and lithologic descriptions are listed in Table 1. A detailed geochemical analysis of these rocks is forthcoming.

Lithologies:

Massive Amphibolite Package: These rocks are medium- to coarse-grained, dark gray to black amphibolites with white plagioclase and quartz foliation bands. Mineralogy includes mainly hornblende and plagioclase with quartz, biotite, garnet, magnetite and chromite as accessories. Hornblende and biotite crystals are oriented parallel to the foliation bands. According to field observations and whole rock chemistry, possible protoliths for the massive amphibolites are basalt flows or tuffs (Table 1).

Metasedimentary Package: Interlayered quartzofeldspathic gneiss, amphibolite, and quartzite comprise this intensely deformed zone.

Quartzofeldspathic Gneiss: This lithology consists of coarse-grained, lensing and laminated biotite-garnet-sillimanite quartzofeldspathic gneiss. Mineralogy includes quartz, plagioclase, alkali feldspar, sillimanite, garnet, biotite, muscovite, chlorite, and zircon. Accessories include cordierite and magnetite. Cordierite, muscovite, and chlorite may represent a late greenschist retrograde event. The foliations consist of alternating bands of biotite-sillimanite layers and quartz-plagioclase layers. Biotite and sillimanite crystals are oriented parallel to foliations and are observed to both wrap around folds and be axial planar in tightly appressed hinge zones. The quartzofeldspathic gneisses are interpreted to represent a metamylonite that was recrystallized during a heating event after the deformation that caused the mylonitic texture. Their geochemistry and the presence of rounded zircon grains suggest a sedimentary protolith.

Amphibolite: These rocks are medium-grained dark gray to black amphibolite layers with white plagioclase foliation bands, interstratified with quartzofeldspathic gneiss and quartzite. Mineralogy is identical to that of the massive amphibolites. Geochemical data and field observation suggests basalt as a possible protolith.

Quartzite: Commonly green with chrome-rich fuchsite, this lithology consists of fine grained quartzite interlayered with amphibolite and gneiss. Minerals include quartz and accessories. A pure quartz sandstone or chemically deposited chert are two possible protoliths based upon geochemistry.

Metaultramafics: These rocks are found in pods of coarse-grained dark gray-green metaultramafic. Minerals include olivine, orthopyroxene, clinopyroxene, and hornblende with traces of biotite, phlogopite and opaques. Most minerals have been altered by a greenschist retrogression causing serpentinization and